Published in final edited form as:
Anal Chem. 2010 January 15; 82(2): 680–688. doi:10.1021/ac902222n.

Effects of Architecture and Surface Chemistry of Three-Dimensionally Ordered Macroporous Carbon Solid Contacts on Performance of Ion-Selective Electrodes

Melissa A. Fierke, **Chun-Ze Lai**, **Philippe Bühlmann***, and **Andreas Stein***
Department of Chemistry, University of Minnesota, 207 Pleasant Street SE, Minneapolis, Minnesota 55455

Abstract

The effects of the architecture and surface chemistry of three-dimensionally ordered macroporous (3DOM) carbon solid contacts on the properties of ion-selective electrodes (ISEs) were examined. Infiltration of the plasticized PVC membrane into the pores of the carbon created a large interfacial area between the sensing membrane and the solid contact, as shown by cryo-SEM and elemental analysis. This large interfacial area, along with the high capacitance of the 3DOM carbon solid contacts (as determined by cyclic voltammetry, chronopotentiometry, and electrochemical impedance spectroscopy) results in an excellent long-term stability of the potentiometric response, with drifts as low as 11.7 μV/h. The comparison of 3DOM carbon solid contacts with an untemplated carbon solid contact shows that the pore structure is an essential feature for the excellent electrode performance. However, the surface chemistry of the 3DOM carbon cannot be ignored. While there is no evidence for an aqueous layer forming between the sensing membrane and unoxidized 3DOM carbon, electrodes based on oxidized 3DOM carbon exhibit potentiometric responses with the typical hysteresis indicative of a water layer. A comparison of the different techniques to characterize the solid contacts confirms that constant-current charge-discharge experiments offer an intriguing approach to assess the long-term stability of solid-contact ISEs but shows that their results need to be interpreted with care.

Introduction

Solid-contact ion-selective electrodes (SC-ISEs) have progressed significantly since the introduction of the coated wire electrode (CWE) in 1971.[1] In CWEs, a sensing membrane is coated directly onto a metal contact. However, while CWEs are capable of short term reproducibility of measurements, they show large long term drifts on the order of several hundred μV/h and higher.[2, 3] This potential instability is due to the 'blocked' interface between the metal contact and sensing membrane, preventing ion and electron transfer across the interface.[4] In order to improve the potential stability and reproducibility of SC-ISEs, various intermediate layers between the metal contact and the sensing membrane have been investigated. Sensors with a hydrogel layer between the metal contact and sensing membrane were shown to exhibit somewhat smaller drifts than a CWE system (e.g., 250 μV/h for pH, 90 μV/h for K^+).[5] However, hydrogels are not truly solid contacts as they are swelled with an

*To whom correspondence should be addressed. Phone: 612-624-1431. Fax: 612-626-7541. buhlmann@umn.edu (P.B.); Phone: 612-624-1802. Fax: 612-626-7541. a-stein@umn.edu (A.S.).

Supporting Information Available
SEM images of 3DOM carbon infiltrated with polymeric membranes containing different percentages of PVC and CV data for 3DOM carbon electrodes in acetonitrile solution are available as supporting information This material is available free of charge via the Internet at http://pubs.acs.org.

electrolyte solution. Moreover, they are hard to miniaturize and suffer from osmotic pressure differences. SC-ISEs with a self-assembled monolayer (SAM) of a redox-active compound as the intermediate layer between the metal contact and sensing membrane were reported to exhibit a drift of 85 μV/h for the detection of K^+.[6] In order to improve the stability even further, materials with a higher redox capacitance than SAMs, such as conducting polymers, were necessary.[7–14] Details of many investigations of conducting polymer systems were discussed in several recent reviews.[15–17] While conducting polymers allowed for improved detection limits and smaller drifts, the choice of polymer can render them sensitive to several interferences, such as from oxygen, pH and light.[18]

Carbon materials were also explored as electrode components in ISEs. Already in the 1970s, early versions of the so-called "selectrodes" were prepared by directly coating the surface of a graphite pellet with an ion-exchanger or ionophore-doped hydrophobic liquid.[19] Long term drifts of such electrodes were not reported, and they were soon replaced by similar constructs in which Hg_2Cl_2 and Hg were admixed to the graphite pellet, giving an E° shift of 22 mV over one week (131 μV/h) for a valinomycin-based selectrode.[20] Carbon materials with a much higher surface area, i.e., three-dimensionally ordered macroporous carbon (3DOM carbon),3, 21 carbon nanotubes,22–25 and fullerenes26 have only been used as solid contacts recently. The fullerene-consisting electrode constructs were reported to show much less drift in the initial conditioning process, but long-term drifts were not described. To prepare SC-ISEs with carbon nanotubes as solid contact, a suspension of single-walled carbon nanotubes (SWCNTs) was sprayed onto a mechanical support. After a sufficient amount of SWCNTs had been deposited, an ionophore-doped polymeric membrane was applied. When a current of 1 nA was applied, chronopotentiometry showed a drift of 61.2 mV/h, which was about 16 times lower than for a CWE system.22 While in individual SWCNTs the carbon atoms are arranged with a very high level of order, a layer of SWCNTs shows no long-range order. In contrast, 3DOM carbon consists of a glassy carbon skeleton surrounding an array of macropores several hundred nanometers in diameter, with a high level of order extending well over the micrometer level. 3DOM carbon is electrically conductive, and the pores can be infiltrated with the ionophore-doped sensing membrane, making it an ideal solid contact material.3 When 3DOM carbon was used as a solid contact between a metal contact and an ionophore-containing plasticized poly (vinyl chloride) (PVC) sensing membrane, excellent results were obtained. The electrodes exhibited Nernstian responses and a high resistance to interference from oxygen and light.3 After optimization, detection limits of 1.6×10^{-7} M and 4.0×10^{-11} M were achieved for K^+ and Ag^+, respectively.[21] In view of long-term measurements without frequent recalibrations, the extremely low long term drifts of 11.7±1.0 μV/h over 70 h were particularly promising.[3]

While these studies demonstrated that 3DOM carbon serves as an excellent solid contact in a SC-ISE system, the reasons for this remarkable performance have not been investigated up to now. We hypothesized that the high capacitance of the solid contact in 3DOM carbon based electrodes and the large interfacial contact area between 3DOM carbon and the sensing membrane led to the performance advantages of these electrodes, and that surface functional groups on the 3DOM carbon surface affected the sensor performance. In the investigation reported here, ISEs with solid contacts prepared from related solid-contact materials (3DOM carbon, oxidized 3DOM carbon, and an untemplated carbon from the same precursor as 3DOM carbon) were studied by cyclic voltammetry, chronopotentiometry, electrochemical impedance spectroscopy, cryo-scanning electron microscopy (cryo-SEM), elemental analysis, titrations to determine the surface chemistry of 3DOM carbon, and potentiometry to measure the initial potential, intermediate-term responses in aqueous layer tests, and long-term drifts.

Experimental

Reagents

High molecular weight PVC and *ortho*-nitrophenyl octyl ether (*o*-NPOE) were purchased from Fluka (Buchs, Switzerland), valinomycin, potassium hexafluorophosphate (99.5%), sodium ethoxide solution (21 wt % in ethanol), and bromocresol green/methyl red (mixed indicator solution in methanol) from Sigma-Aldrich (St. Louis, MO), NaOH and Na_2CO_3 solutions from Alfa Aesar (Ward Hill, MA), $NaHCO_3$ and HCl from Mallinckrodt Baker (Paris, KY), unplasticized PVC sheet as substrate from Goodfellow (Oakdale, PA), and sodium tetrakis[3,5-bis(trifluoromethyl)phenyl]borate (NaTFPB) from Dojindo (Kumamoto, Japan). Ni mesh was a gift from Dexmet (Branford, CT). Deionized and charcoal-treated water (18.2 MΩ·cm specific resistance) was used for all sample solutions. All chemicals were used as received.

Solid Contact Synthesis

The 3DOM carbon solid contact was prepared as previously described.[3] A resorcinol-formaldehyde precursor was infiltrated into a colloidal crystal template (here, an ordered array of poly(methyl methacrylate) spheres). After curing at 85° for 3 days to crosslink the precursor, the sample was pyrolyzed at 900 °C under flowing nitrogen to convert the precursor to glassy carbon and remove the template. Untemplated glassy carbon samples were prepared by following the same procedure as for the 3DOM carbon but excluding the template. Oxidized 3DOM carbon was prepared by boiling 3DOM carbon monoliths in concentrated nitric acid at 130 °C for 10–60 min, followed by thorough washing with DI water. 3DOM carbon, oxidized 3DOM carbon, and untemplated carbon solid contacts were affixed to Ni mesh metal contacts using resorcinol-formaldehyde carbon precursor that had been heated for approximately 20 min to make it more viscous, followed by curing at 85 °C overnight. Unoxidized and oxidized 3DOM carbon samples had dimensions of approximately 5×5×0.5 mm^3, while untemplated samples had dimensions of approximately 5×5×1 mm^3.

Preparation of Sensing Membranes

K^+ selective sensing membranes were prepared as previously described.[3, 21] THF solutions of the membrane components (200 mg) were poured into glass dishes with an inner diameter of 31 mm, and the THF was allowed to evaporate overnight. The membranes were composed of 33–75 wt % polymer (PVC), 0.6 wt % ionic sites (NaTFPB), 1.0 wt % ionophore (valinomycin), and the remainder plasticizer (*o*-NPOE).

Electrode Preparation

To prepare the electrodes, part of the Ni mesh of the solid contact/nickel mesh constructs was sealed in between two pieces of unplasticized PVC, using THF and a commercially available PVC cement as adhesive. The 3DOM carbon was covered with a PVC membrane, and the edges of the membrane were glued to the PVC sheet with THF. The electrodes were conditioned in 0.1 M KCl overnight.

Characterization

EMF Measurements

Electrode potentials were measured with 2.5 μV resolution with an EMF 16 potentiometer controlled with EMF Suite 1.02 software (Lawson Labs, Malvern, PA). All measurements were performed in stirred solutions at room temperature. A double-junction Ag/AgCl reference electrode with a 1.0 M LiOAc bridge electrolyte and AgCl-saturated 3.0 M KCl inner reference electrolyte was used. All EMF values were corrected for liquid-junction potentials using the Henderson equation.27 A two-parameter Debye-Hückel approximation was used to calculate

activity coefficients.28 Measurements of long-term stability were performed with a temperature-controlled cell using a water bath (25 °C).

Electrochemical Impedance Spectroscopy

All impedance experiments were performed on a Solartron 1255B Frequency Response Analyzer with a SI 1287 Electrochemical Interface (Farnborough, Hampshire, UK) controlled by ZPlot software (Scribner Associates, Southern Pines, NC). ZView software was used to view and fit the data. The typical frequency range for the measurement was 200 kHz to 0.1 Hz. Measurements were performed at open circuit potential with an AC amplitude of 10 mV.

Measurements were performed under aqueous or non-aqueous conditions, depending on the type of electrode. For aqueous systems, a 0.1 M KCl solution was used as the electrolyte, with a double-junction Ag/AgCl reference electrode (with a 1.0 M LiOAc bridge electrolyte and AgCl-saturated 3.0 M KCl inner reference electrolyte) or a Ag/AgCl Luggin capillary filled with 3.0 M KCl. For non-aqueous systems, a 0.1 M solution of KPF_6 in acetonitrile was used as electrolyte, and a Luggin capillary filled with 3.0 M KCl was used as reference electrode. In all cases, a platinum wire served as the counter electrode.

Capacitance Measurements

To ensure complete wetting of the carbon during the capacitance experiments, a non-aqueous electrolyte (0.1 M KPF_6 in acetonitrile) was used. The non-aqueous reference electrode was a Ag wire in 0.1 M $AgPF_6$ in acetonitrile. A three-electrode setup was used for all experiments, with the carbon electrode as the working electrode, a Pt wire as the counter electrode, and the non-aqueous reference electrode. All experiments were carried out in a closed three-neck flask, and the electrolyte solution was purged with argon for at least 15 minutes prior to each measurement.

For cyclic voltammetry experiments, a potential window of 0.6 V centered around 0.0 V with a scan rate of 0.5 mV/s was used. Three cycles were typically used, and the capacitance value was obtained from the third cycle. The capacitance was calculated by averaging the absolute value of the two current values at the center of the positive and negative sweep (typically 0.0 V). This average current was then divided by the scan rate and the mass of the electrode, giving a capacitance value in F/g.

For chronopotentiometry (which may also be referred to as constant current charge-discharge) experiments, a constant current was applied to the electrode until an upper potential limit was reached (charge), at which time an equal but opposite current was applied until a lower potential limit was reached (discharge). The upper and lower potential limits were typically 0.2 V and 0.0 V, respectively, for unoxidized carbon and 0.7 V and 0.0 V, respectively, for oxidized carbon. The capacitance in F/g was determined by dividing the applied current by the mass of the electrode and by the slope of the discharge line in a potential vs. time graph.

All cyclic voltammetry experiments were performed on an Electrochemical Analyzer (CH Instruments, Inc.; Austin, TX). All charge/discharge experiments were performed on a Solartron 1255B Frequency Response Analyzer with a SI 1287 Electrochemical Interface.

Scanning Electron Microscopy

For carbon not infiltrated with a PVC membrane, the samples were affixed on an aluminum stub with conductive carbon tabs. Imaging was carried out on a JEOL 6700 field emission gun scanning electron microscope with an accelerating voltage of 5.0 kV.

Cryo-Scanning Electron Microscopy

Due to the volatility of *o*-NPOE in high vacuum, electrodes were imaged using cryo-SEM on a Hitachi S-4700 cold field emission gun scanning electron microscope with an accelerating voltage of 3.0 kV. To prepare the electrodes for imaging, the membrane-covered pieces of 3DOM carbon were removed from the PVC substrate and Ni mesh metal contact. The membrane-covered carbon was mounted in the sample holder, which was then submerged in liquid nitrogen for quick freezing. From this point forward, the sample holder remained at liquid nitrogen temperature during the entire imaging process. After several minutes, the sample holder was transferred to a vacuum chamber and evacuated. The electrode was fractured to reveal a fresh cross section. A thin layer of Pt was then sputtered onto the membrane-coated carbon to improve its conductivity for imaging. The sample holder was transferred under vacuum to the microscope for imaging.

Elemental Analysis

C, H, N, O, and Cl elemental analyses were performed by Atlantic Microlab (Norcross, GA). For electrodes containing PVC membranes, the outer PVC membrane layer was removed prior to analysis and three electrodes were combined to supply sufficient material for each elemental analysis set.

Acid Base Titrations to Determine Surface Functionality

The quantity of oxygen-containing surface functional groups was determined by a modified version of a published acid/base titration procedure.[29, 30] Unoxidized 3DOM carbon and 3DOM carbon that had been oxidized for 10, 30 and 60 minutes were ground to powders to allow better mixing with the base solutions. The carbon samples were dried at 100 °C overnight, mixed with base, and then the excess of base was back-titrated with 0.025 M HCl using a mixed methyl red/bromocresol green end point indicator. Four types of base solutions were used to determine different types of surface functional groups: aqueous solutions of NaOH, Na_2CO_3, and $NaHCO_3$, as well as an ethanol solution of sodium ethoxide (all 0.05 M). In order to enhance the infiltration of the base solutions into the carbon, they were mixed under static vacuum. For each of the four carbon types (unoxidized and 10-, 30- and 60-min oxidations), four 60 mg samples were placed in small plastic bottles and sealed with rubber septa. The bottles were then evacuated for 15 min, refilled with nitrogen, and evacuated for 15 more minutes. Then, 25 mL of a base solution was injected into each bottle using a syringe. The carbon was soaked in the base solutions for two days, swirling occasionally. After soaking, the base solutions were recovered by filtering the solutions through a 0.2 μm syringe filter and back-titrated.

Nitrogen Sorption

Nitrogen sorption measurements were carried out at 77 K. The unoxidized sample was evaluated after degassing overnight at 150 °C to 40 Pa using a Micromeritics ASAP 2000 system; the oxidized samples were tested on a Quantachrome Instruments Autosorb-1 system after degassing overnight at 150 °C to 13 Pa. The Brunauer-Emmett-Teller (BET) method was applied to calculate specific surface areas, and the pore sizes and volumes were estimated from the pore size distribution curves obtained from the adsorption branches of the isotherms.

Results and Discussion

K^+ selective electrodes were prepared by affixing a valinomycin-containing plasticized PVC sensing membrane over carbon solid contacts attached to a Ni mesh as metal contact. As in our previous work,[3, 21] 3DOM carbon, with walls of glassy carbon surrounding an array of interconnected macropores, was the primary solid contact used. For comparison, oxidized 3DOM carbon and an untemplated carbon prepared from the same precursor as the 3DOM

carbon were also used as solid contacts for polymeric sensing membranes. The properties of the ISEs with 3DOM carbon solid contacts were investigated by examining their structure, capacitance, and the surface chemistry of the unoxidized and oxidized 3DOM carbon, and by performing electrochemical impedance spectroscopy on several types of electrode constructs.

Electrode Structure

Cryo-SEM analysis of 3DOM carbon/PVC electrodes was performed to ensure that the plasticized PVC membranes wet the carbon monoliths, and to qualitatively evaluate the degree of infiltration of the membranes into the pores of the carbon. SEM images of pristine 3DOM carbon and an electrode with a sensing membrane containing 33 wt % PVC are shown in Figure 1. SEM images of electrodes with sensing membranes containing 43 and 66 wt % PVC are provided in Figure S1 (see Supporting Information). The sensing membranes coat the pore walls of each monolith and in some cases completely fill part of the pore structure, creating a bicontinuous carbon/membrane structure. For all electrodes, the plasticized polymer is distributed throughout the entire thickness of the monolith, facilitating charge transport through the entire construct. Importantly, the penetration of the polymeric phase deep into the porous 3DOM carbon provides a large interfacial area between the polymeric sensing membrane and the carbon.

However, by examination of the cryo-SEM images alone, it is not possible to determine whether the infiltrated membrane has the same composition as the prepared membrane, or whether the membranes de-mix and one component (PVC or plasticizer) preferentially enters the 3DOM carbon monoliths. Therefore, elemental analysis was performed on electrodes whose outer membrane layer had been removed in order to determine the composition of the membrane that had infiltrated into the 3DOM carbon monoliths. For this purpose, electrodes fabricated with sensing membranes containing 33, 43, 66 and 74 wt % polymer were analyzed. Elemental analysis data of bare 3DOM carbon (without PVC membrane) are provided in Table 1 for comparison. The chlorine and nitrogen contents were used to determine the compositions of the infiltrated membranes since chlorine and nitrogen are present only in the PVC and the plasticizer *o*-NPOE, respectively. While the PVC content of the as-prepared membranes ranged from 33–74 wt %, the PVC content of the infiltrated membranes ranged from 11–54 wt % (see Table 1). The actual PVC contents of the infiltrated membrane material are lower for each system than for the as-prepared membranes, with the largest difference in the electrode with 33 wt % PVC in the as-prepared membrane. This shows that during the preparation of the electrodes, the membranes de-mix, with the lower viscosity component *o*-NPOE preferentially entering the pores of the carbon. Indeed, separation of plasticizer and PVC in ISE sensing membranes has previously been observed at the surface of similar types of membranes.[31, 32] However, in the case of the 3DOM carbon electrodes, the limited extent of demixing ensures that PVC enters the pores of the solid contact, thereby inhibiting delamination of the sensing membrane overlayer.

The elemental analysis data was also used to estimate the extent of infiltration of the sensing membrane material into the 3DOM carbon monoliths. The filling fraction of the sensing membrane material in the pores of the 3DOM carbon monolith was obtained for each of the different membrane compositions. Volume fractions of 26% carbon and 74% macropore volume were assumed for the 3DOM carbon solid contact (the theoretical values for a face-centered cubic array of spheres). The densities of 3DOM carbon, PVC, and *o*-NPOE as well as the PVC content of the infiltrated membranes (as calculated above and shown in Table 1) were used to estimate the filling fraction of the membrane in the void space of the 3DOM carbon skeleton. The filling fraction decreased as the PVC content of the membrane increased, ranging from 25% for the as-prepared membrane containing 33 wt % PVC to approximately 9% for the as-prepared membranes containing 43, 66, and 74 wt % PVC. Importantly, as shown

by the cryo-SEM data discussed above, this membrane material in the voids is coating the surface of the 3DOM carbon pores. Even though one may conceive of methods of filling the pores to a greater extent, here we chose to use the same methods as in our previous studies[3, 21] to help our understanding of the excellent performance of this system.

Surface Chemistry of 3DOM Carbon

In order to investigate if there is a relationship between the initial potential (E°) of the electrodes and the surface chemistry of the 3DOM carbon, E° of SC-ISEs with 3DOM carbon contacts containing different amounts of surface functional groups was measured. For this purpose, a series of 3DOM carbon samples oxidized for varying amounts of time (0, 10, 30 and 60 min) was prepared. Oxidation of the 3DOM carbon increases the overall surface area and pore volume, largely through the generation of new micropores (Table 2). Acid/base titrations with four different bases were used to determine the quantity of different oxygen-containing surface functional groups for each sample by mixing each base with the 3DOM carbon and allowing them to react with the surface functional groups. After filtering the carbon out, the bases were back-titrated to determine the change in concentration. As Table 3 shows, the number of surface functional groups increases with the time of 3DOM carbon oxidation. The largest increase is observed in the number of carboxylic acid groups, which can provide the surface with negative charges.

Four sets of electrodes with 3DOM carbon solid contacts with different levels of oxidation (0, 10, 30 and 60 min) were fabricated with sensing membranes containing 33 wt % PVC (three or four electrodes for each oxidation level). Each set of electrodes was prepared using the same master membrane, and each of the four master membranes was prepared in an identical manner from the same THF solution of the membrane components. The average E° value for each set of electrodes (after conditioning) is shown in Table 3. The initial potential for electrodes prepared with oxidized carbon is higher than that of the electrodes prepared with unoxidized carbon. While the ranges of the E° values for electrodes with the same level of 3DOM carbon oxidation are rather small in comparison to the difference in E° for the different levels of oxidation, no direct relationship between oxidation time and initial potential is apparent.

Aqueous Layer Test and Long-term Drift

The formation of an aqueous layer between the ion-selective sensing membrane and solid contact is directly related to the surface chemistry of the solid contact. If such a layer is formed, it can significantly affect the response and detection limit of a SC-ISE, and in the case of conventional SC-ISEs it can lead to complete delamination of the sensing membrane from the solid contact.[33, 34] To test for the formation of an aqueous layer, we used in our previous work unoxidized 3DOM carbon-contacted electrodes and monitored the potential when changing from an initial conditioning solution (100 mM KCl) to 100 mM NaCl, followed by a switch back to the conditioning solution.[3] Negative potential drift when changing back from the interfering ions to primary ions would indicate the presence of a water layer,[33] but no such drift could be observed for the 3DOM carbon constructs. The only indication that the 3DOM carbon construct may not be perfectly ideal was the observation of 4 mV difference in the EMF before and after the exposure to the Na^+ solution.

For this work, oxidized 3DOM carbon and untemplated carbon-contacted electrodes were examined using the same procedure (Figure 2). A very large negative drift was observed for the untemplated carbon-contacted electrode. This is clear evidence for the formation of an aqueous layer between untemplated carbon and the PVC membrane, and it is likely also related to the very poor long-term stability of this system with a potential drift of 1530 μV/h over 70 h.

Evidence for the existence of an aqueous layer was also found for the oxidized 3DOM carbon-contacted electrode, even though the overshoot in potential was smaller than for the untemplated carbon. After going through a maximum, the EMF gradually decreased by 11.9 mV until it stabilized at a value 9.4 mV lower than before exposure to the Na^+ solution.

The worse performance of the oxidized 3DOM carbon as compared to the unoxidized 3DOM carbon is consistent with the different potential stabilities of the two systems. The average drift for three SC-ISEs with an unoxidized 3DOM carbon solid contact after initial conditioning in K^+ solution for 24 h was found to be 11.7±1.0 μV/h over 70 h.[3] For three SC-ISEs with an oxidized 3DOM carbon solid contact, drifts of 29±33 μV/h were determined. While even the drifts for the oxidized 3DOM carbon constructs are small, they are larger than for the unoxidized 3DOM carbon. The large increase in surface area resulting from the introduction of macropores allows for a much larger interfacial surface area between the solid contact and sensing membrane, leading to a much lower drift compared to the untemplated carbon. However, increasing the surface area further by oxidation of the carbon does not lead to a further increase in stability. The corresponding surface area increase is mostly due to micropores (<2 nm), which are not readily accessible to all membrane components. Also, the oxidation causes a significant increase in the concentration of oxygen-containing functional groups (as shown above), creating a more hydrophilic surface. This allows for the formation of a water layer, decreasing the stability of the electrodes.

Electrochemical Investigation of 3DOM Carbon Solid Contacts

Several electrochemical techniques were used to examine unoxidized 3DOM carbon and oxidized 3DOM carbon solid contacts in order to better understand their effect on potentiometric measurements. First, cyclic voltammetry (CV) was performed on unoxidized 3DOM carbon and 3DOM carbon that had been oxidized for 15 min. The measurements were performed without polymeric sensing membranes and using acetonitrile as the solvent (0.1 M KPF_6), which effectively wets both types of carbon. A scan rate of 0.5 mV/s was used, and the capacitance was calculated from the current values at 0.0 V of the last cycle (see Experimental Section). The measured capacitance of unoxidized 3DOM carbon was 3.9 F/g, whereas the value for oxidized 3DOM carbon was 62 F/g. The large increase in capacitance after oxidation cannot be explained only by the increase in surface area associated with the oxidation (Table 2). Oxidation for 15 min increased the surface area of the 3DOM carbon by about 50% while the apparent capacitance as determined by CV increased by a factor of 16.

The same trend was also observed when capacitances were determined using chronopotentiometry with unoxidized and oxidized 3DOM carbon (15 min oxidation) in acetonitrile solution at three different currents (1, 0.5 and 0.1 mA, see Table 4 and Figure 3). For unoxidized carbon, the capacitance increased from 1.92 to 2.25 F/g as the current decreased from 1 to 0.1 mA. For oxidized carbon, this effect was even more pronounced. The apparent capacitance increased from 11.0 to 68.4 F/g when the current was decreased from 1 to 0.1 mA. As for the cyclic voltammetry, the timescale of the experiment appears to have a large effect on the capacitance, especially for oxidized 3DOM carbon. This suggests that a technique with time resolution, such as electrochemical impedance spectroscopy (EIS),[35, 36] is better suited to characterize the capacitance of 3DOM carbon electrodes.

Therefore, EIS was performed on unoxidized 3DOM carbon (again in acetonitrile solution). The complex plane plot and fitted equivalent circuit are shown in Figure 4A, while the values of the fit are shown in Table 5. In the fit for this construct, the series resistance R1 arises from the acetonitrile solution and the Luggin capillary reference electrode. The observation of a parallel combination of a capacitor and resistor (C1/R2) is expected for an electrode surface exhibiting interfacial capacitance (C1) and interfacial charge transfer resistance (R2), and is associated in this case with the surface of the 3DOM carbon. Since the series combination of

R1 and C1/R2 did not provide a good fit, an additional parallel combination of a resistor (R4) and a constant phase element (CPE1) was used for fitting. CPEs with a phase value of 1.0 behave as capacitors, while CPEs with a phase value of 0.5 behave as Warburg impedances.[36] In this case, the fitted phase value of 0.37 suggests that the CPE1/R4 element appears to be associated with Warburg diffusion and that R4 represents the resistance of the electrolyte phase trapped within the 3DOM carbon. Note that data for ω>1500 Hz were not used for this fit since they are part of a semicircle centered on the negative side of the×axis and can be readily recognized as affected by a high frequency instrumental artifact.37

If the mass of the 3DOM carbon monolith used for the EIS shown in Figure 4A is taken into account, a specific capacitance of 1.77 F/g is obtained from the fitted value of C1. This value is reasonably close to the one obtained for unoxidized 3DOM C using CV (3.9 F/g) and chronopotentiometry at 1 mA (1.92 F/g). However, since EIS takes advantage of the frequency dependence to distinguish between the C1/R2 and CPE1/R4 elements, the value of 1.77 F/g for non-oxidized 3DOM carbon appears to be most trustworthy.

The larger values for the apparent capacitance values obtained from CV or chronopotentiometry, in particular when investigated in long experiments (i.e., for slow scan rates in CV and for low currents in chronopotentiometry), and the much larger apparent capacitances for oxidized 3DOM carbon can be explained by the occurrence of redox reactions. In the case of CV, they increase the total current beyond the double layer charging current. In the case of chronopotentiometry, they reduce the fraction of the total current available to charge the double layer. While the chronopotentiometry data look symmetrical with respect to charging and discharging, the CVs clearly lack symmetry with respect to the direction of the scan (See Figure S2, Supporting Information). This indicates that the redox reactions in question are irreversible on the CV time scale. The much higher apparent capacitance in the case of the oxidized 3DOM carbon despite the only marginally increased surface area suggests that the rate of these redox reactions is directly affected by the surface functional groups. This may be explained by redox reactions that involve these functional groups themselves. Alternatively, these functional groups may play a catalytic role. Indeed, a strong dependency of the rate constants of redox reactions on the surface chemistry of carbon electrodes is well known.[38]

EIS Investigation of PVC Membrane-Coated Electrode Constructs

Four membrane-coated electrode constructs were also investigated using EIS: a piece of Ni mesh covered with a PVC sensing membrane in order to characterize electrodes without a carbon solid contact, and three PVC sensing membrane-covered electrodes with different carbon solid contacts (3DOM carbon, 3DOM carbon oxidized for 15 min, and untemplated carbon) in order to examine the effects of different solid contacts. For all PVC membrane-coated constructs, an aqueous electrolyte containing K^+ was used. The complex plane impedance plot for each system (Figures 4B–E) was fitted to an equivalent circuit (insets of Figure 4, fit values in Table 5).

All four constructs are more similar to each other than they are to the system without a PVC membrane, as it was described above. In each case, a negative R1 values is observed. Similarly as for the membrane-free constructs, this is an instrumental high frequency artifact. For all four electrodes, the fits provide an R2 value of a few hundred kΩ, which is a value very typical for bulk resistances of plasticized PVC membranes. Consequently, the C1 element represents the geometrical capacity of the sensing membranes. Similar semicircles arising from a parallel combination of C1/R2 have been observed in numerous impedance studies of ISEs.[31, 35] For all four PVC membrane-coated electrode constructs, the CPE1/R4 element (or alternatively the CPE1 element, which is equivalent with a CPE/R element with a very large resistance R) corresponds to the CPE1/R4 element in the 3DOM carbon case. Here, this term is associated

with diffusion through the bulk of the PVC membrane that is the top layer of the four electrode constructs instead of diffusion through the organic electrolyte, as for the 3DOM carbon constructs without polymeric sensing membrane. Therefore, R4 has a much larger value than in the case of the 3DOM carbon in acetonitrile electrolyte solution (i.e., without polymeric membrane coating). While for the Ni/PVC electrode and the construct with the untemplated carbon the phase values for the CPE differ more significantly from 0.5, the more important cases of the constructs with non-oxidized and oxidized 3DOM carbon are characterized by phase values very close to 0.5, as it is expected for a pure Warburg impedance.

In the cases where the solid contacts are 3DOM carbon (oxidized or not; Figures 4D and 4C, respectively), an additional element (C2/R3) is present. The fitted value of the C2 is very similar to the fitted values of C1 for the geometrical capacitance of the polymeric sensing membrane located on top of the 3DOM carbon constructs, and indeed many orders of magnitude smaller than the double layer capacitance of the 3DOM carbon surface, as observed in Fig. 4A. We conclude that C2, and therefore R3, are both associated with the plasticized polymeric membrane material within the pores of the 3DOM carbon. The lower resistance R3 for the oxidized 3DOM carbon as compared to the unoxidized 3DOM carbon is consistent with its larger available pore volume (see Table 2). The overlap of the two semicircles for C1/R2 and C2/R3 due to the similar values of C1 and C2 as well as R2 and R3 explain the semi-ellipse feature in the impedance plots in Figures 4C and 4D. This particular shape is distinctly different from the nearly ideal semi-circles observed for Figures 4B and 4E and appears to be characteristic for the electrodes with 3DOM carbon (whether unoxidized or oxidized) solid contacts. Its observation is a further confirmation for the penetration of the polymeric sensing membrane material into the porous 3DOM carbon.

Conclusions

The structural and electrochemical properties of K^+ ISEs with 3DOM carbon, oxidized 3DOM carbon, and untemplated carbon as solid contacts were examined to explain the excellent performance of these SC-ISEs, and, in particular, the very low long-term drift of the potentiometric responses. Cryo-SEM, elemental analysis and EIS confirmed that the components of the sensing membrane enter the macropores of the 3DOM carbon, creating a large contact area between the carbon and the membrane. This large interfacial area, along with the high capacitance of the 3DOM carbon solid contacts as determined by CV, chronopotentiometry, and EIS is essential for the excellent long-term stability. The untemplated carbon, which differs from the unoxidized 3DOM carbon only by its lack of pores, has a much lower surface area and smaller capacitance than either unoxidized or oxidized 3DOM carbon. Electrodes prepared with untemplated carbon show poor initial potential reproducibility and long-term stability. Clearly, the pore structure plays an essential role in determining the properties of the system. However, the surface chemistry of the 3DOM carbon cannot be neglected. The oxidized 3DOM carbon was determined to have a much higher concentration of surface functional groups than the unoxidized 3DOM carbon. While electrodes with oxidized 3DOM carbon as the solid contact had still high long-term stabilities —albeit not as good as SC-ISEs with unoxidized 3DOM carbon contacts—they fared less favorably in the aqueous layer test.

This work also permits a comparison of methods for the characterization of SC-ISEs. There is still little consensus on how to do this best,[17] which can be partially explained by the diversity of their applications. Whereas a quick response and reproducibility of E° are important for single use devices, low drift is essential for long-term monitoring. In view of the latter, constant-current charge-discharge experiments offer an attractive approach to quantify the stability of SC-ISEs because they are fast and are hardly affected by temperature changes and drifts in liquid junction potentials at the reference electrode. However, this work demonstrates that such

experiments can be biased by irreversible redox reactions, which may not be representative of the electrode behavior in long-term potentiometric measurements but are an artifact of the large applied currents. Consequently, charge-discharge experiments need to be interpreted with care.

Supplementary Material

Refer to Web version on PubMed Central for supplementary material.

Acknowledgments

This work was supported by the National Science Foundation (CTS-0428046, EXP-SA 0730437), the National Institute of Health (R01 EB005225-01), the Office of Naval Research (ONR, Grant N00014-07-1-0608) and the MRSEC program of the NSF (DMR-0212302 and DMR-0819885). The authors thank Chris Frethem for his assistance in obtaining the cryo-SEM images, Zhiyong Wang and Won Cheol Yoo for obtaining the nitrogen sorption data, Michael Tsapatsis for the use of the nitrogen sorptometer, and the Dexmet Corporation for providing the Ni mesh. M. A. F. thanks 3M for a Science and Technology Fellowship and the University of Minnesota Graduate School for a Graduate School Fellowship. C.-Z. L. thanks the University of Minnesota for a Louise T. Dosdall fellowship.

References

1. Cattrall RW, Freiser H. Anal. Chem 1971;43:1905–1906.
2. Cattrall RW, Drew DM, Hamilton IC. Anal. Chim. Acta 1975;76:269–277.
3. Lai C-Z, Fierke MA, Stein A, Bühlmann P. Anal. Chem 2007;79:4621–4626. [PubMed: 17508716]
4. Buck, RP. Ion-Selective Electrodes in Analytical Chemistry. Freiser, H., editor. Vol. Vol. 1. New York and London: Plenum Press; 1978. p. 1-142.
5. Cosofret VV, Erdosy M, Johnson TA, Buck RP. Anal. Chem 1995;67:1647–1653.
6. Fibbioli M, Bandyopadhyay K, Liu S-G, Echegoyen L, Enger O, Diederich F, Bühlmann P, Pretsch E. Chem. Commun 2000:339–340.
7. Bobacka J. Anal. Chem 1999;71:4932–4937.
8. Bobacka J, McCarrick M, Lewenstam A, Ivaska A. Analyst (Cambridge, U. K.) 1994;119:1985–1991.
9. Cadogan A, Gao Z, Lewenstam A, Ivaska A, Diamond D. Anal. Chem 1992;64:2496–2501.
10. Chumbimuni-Torres KY, Rubinova N, Radu A, Kubota LT, Bakker E. Anal. Chem 2006;78:1318–1322. [PubMed: 16478128]
11. Gyurcsanyi RE, Rangisetty N, Clifton S, Pendley BD, Lindner E. Talanta 2004;63:89–99. [PubMed: 18969406]
12. Michalska A. Electroanalysis 2005;17:400–407.
13. Michalska A, Konopka A, Maj-Zurawska M. Anal. Chem 2003;75:141–144. [PubMed: 12530830]
14. Sutter J, Pretsch E. Electroanalysis 2006;18:19–25.
15. Bobacka J. Electroanalysis 2006;18:7–18.
16. Bobacka J, Ivaska A, Lewenstam A. Chem. Rev. (Washington, DC, U.S.) 2008;108:329–351.
17. Lindner E, Gyurcsanyi RE. J. Solid State Electrochem 2009;13:51–68.
18. Lindfors T. J. Solid State Electrochem 2009;13:77–89.
19. Ruzicka J, Lamm CG, Tjell JC. Anal. Chim. Acta 1972;62:15–28.
20. Fiedler U, Ruzicka J. Anal. Chim. Acta 1973;67:179–193.
21. Lai C-Z, Joyer MM, Fierke MA, Petkovich ND, Stein A, Bühlmann P. J. Solid State Electrochem 2009;13:123–128. [PubMed: 20046876]
22. Crespo GA, Macho S, Rius FX. Anal. Chem 2008;80:1316–1322. [PubMed: 18271511]
23. Crespo GA, Macho S, Bobacka J, Rius FX. Anal. Chem 2009;81:676–681. [PubMed: 19093752]
24. Mousavi Z, Bobacka J, Lewenstam A, Ivaska A. J. Electroanal. Chem 2009;633:246–252.
25. Zhu J, Qin Y, Zhang Y. Electrochem. Commun 2009;11:1684–1687.
26. Fouskaki M, Chaniotakis N. Analyst (Cambridge, U.K.) 2008;133:1072–1075.
27. Morf, WE. The Principles of Ion-Selective Electrodes and of Membrane Transport. New York: Elsevier; 1981.

28. Meier PC. Anal. Chim. Acta 1982;136:363–368.
29. Boehm H-P, Diehl E, Heck W, Sappok R. Angew. Chem., Int. Ed 1964;3:669–677.
30. Wang Z, Ergang NS, Al-Daous MA, Stein A. Chem. Mater 2005;17:6805–6813.
31. Toth K, Graf E, Horvai G, Pungor E, Buck RP. Anal. Chem 1986;58:2741–2744.
32. Ye Q, Borbely S, Horvai G. Anal. Chem 1999;71:4313–4320.
33. Fibbioli M, Morf WE, Badertscher M, De Rooij NF, Pretsch E. Electroanalysis 2000;12:1286–1292.
34. De Marco R, Veder J-P, Clarke G, Nelson A, Prince K, Pretsch E, Bakker E. Phys. Chem. Chem. Phys 2008;10:73–76. [PubMed: 18075683]
35. Pejcic B, De Marco R. Electrochim. Acta 2006;51:6217–6229.
36. Orazem, ME.; Tribollet, B. Electrochemical Impedance Spectroscopy; Wiley-Interscience. Hoboken, NJ: 2008.
37. Vanysek P. ECS Trans 2008;13:101–113.
38. McCreery RL. Chem. Rev. (Washington, DC, U.S.) 2008;108:2646–2687.

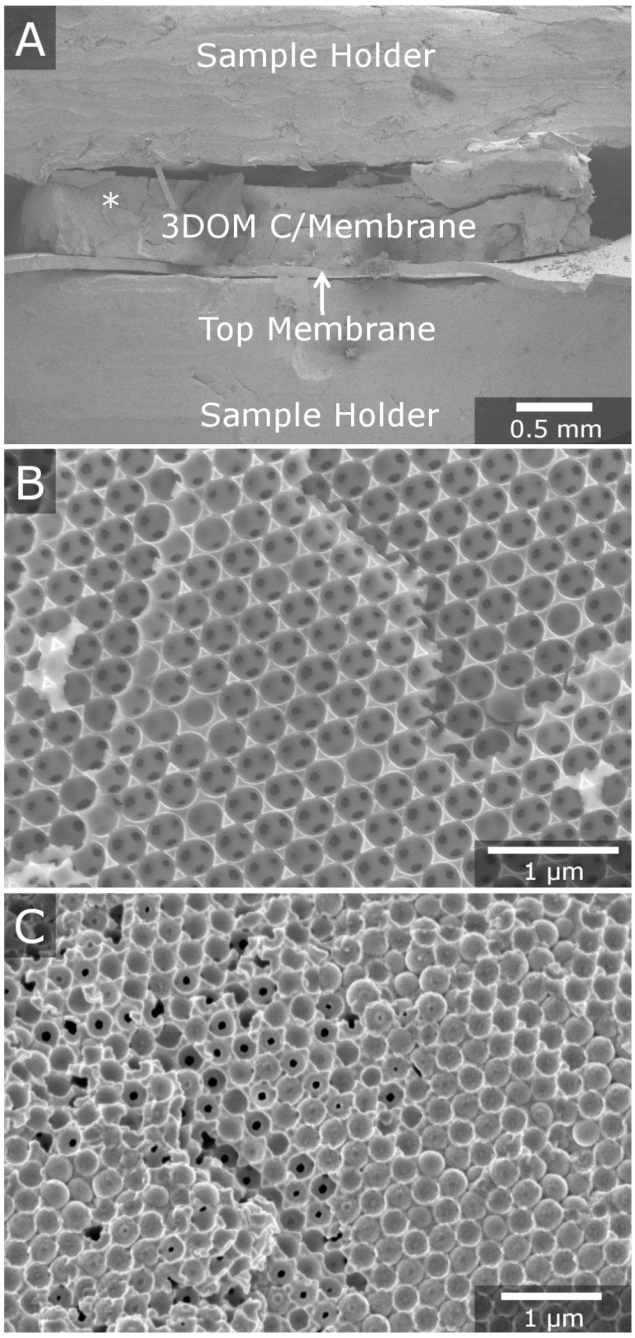

Figure 1.
SEM images of (A) a membrane-infiltrated 3DOM carbon electrode mounted in a sample holder and cross-sections of 3DOM carbon without (B) and with (C) the infiltrated sensing membrane material. The labels in (A) indicate the locations of the membrane-infiltrated 3DOM carbon electrode and the top membrane sandwiched in the sample holder. The * indicates the location from which image (C) was obtained. The PVC content in the as-prepared sensing membrane in (C) was 33 wt %. SEM images of electrodes with as-prepared PVC contents of 43 and 66 wt % are available in Figure S1 of the Supporting Information.

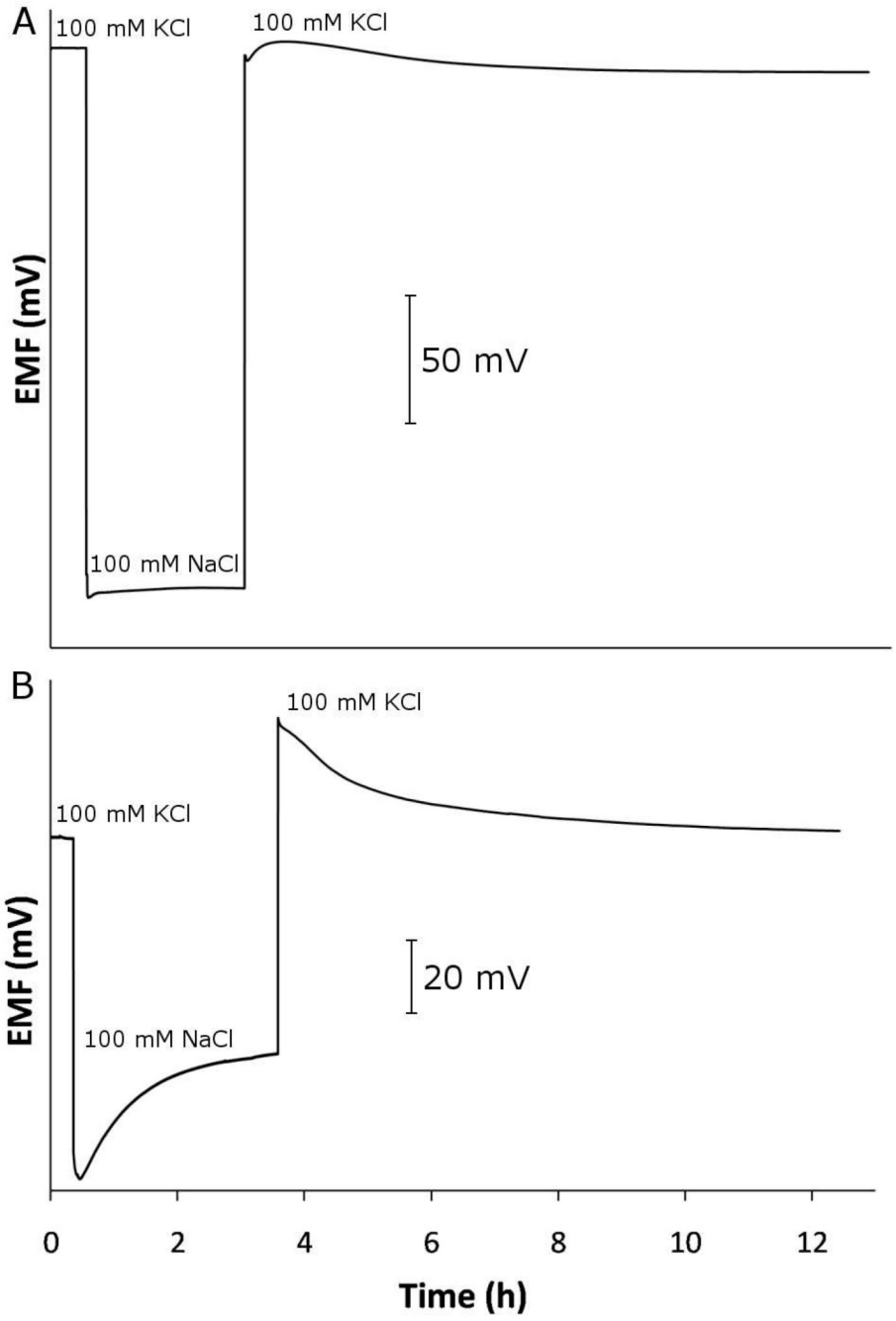

Figure 2.

Aqueous layer test for (A) oxidized 3DOM carbon and (B) untemplated carbon. At t = 0.35 h (for A) or 0.55 h (for B), the 100 mM KCl conditioning solution was replaced by 100 mM NaCl. At t=3.6 h (for A) or 3.0 h (for B), the 100 mM NaCl was replaced by 100 mM KCl.

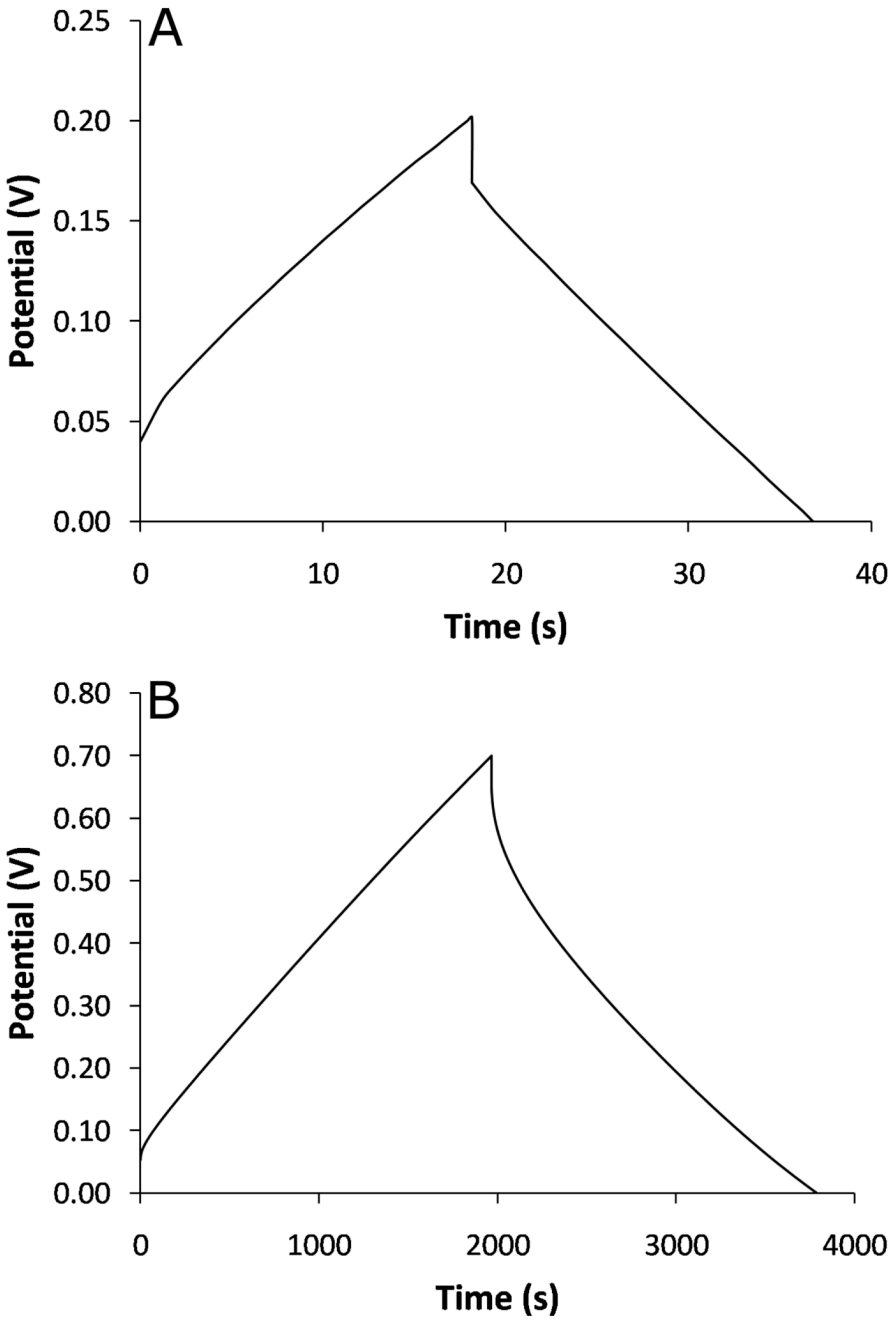

Figure 3.

Chronopotentiometry data for (A) unoxidized and (B) oxidized 3DOM carbon. A charge and discharge current, *i*, of 0.1 mA was used. The instantaneous drops in potential at the peak maxima coincide with the current reversal. They are a result of the cell resistance, *R*, which adds a contribution of *i R* to the observed potential; the sign of this contribution depends on the direction of the current.

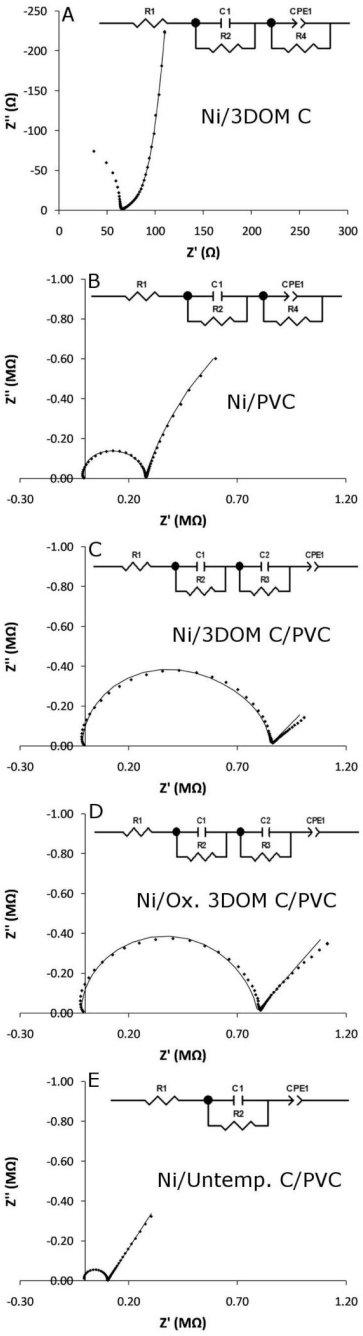

Figure 4.

Complex plane impedance plots and fits of (A) Ni mesh/3DOM carbon in a non-aqueous electrolyte; (B) Ni mesh/PVC membrane; (C) Ni mesh/3DOM C/PVC membrane; (D) Ni mesh/oxidized 3DOM C/PVC membrane (15 min oxidation time); (E) Ni mesh/untemplated carbon/PVC membrane. Data for B–E collected with aqueous electrolyte (0.1 M KCl). Proposed equivalent circuits are shown as insets in each panel. Actual data are shown as ♦, while solid lines represent data fits. The fitted values for the elements of the equivalent circuits are listed in Table 5. Note Ω scale of (A) and MΩ scale of B–E.

Table 1

Elemental analysis data for 3DOM carbon constructs upon infiltration with polymeric sensing membranes of varying PVC contents (3 samples for each PVC content) and for 3DOM carbon without a PVC membrane as a comparison.

PVC content in as-prepared membrane (wt %)	C[a] (wt %)	H (wt %)	N (wt %)	O (wt %)	Cl (wt %)	PVC content in infiltrated membrane (wt %)[b]
(3DOM C only)	92.95	0.27	0.00	2.13	–	–
33	81.02	2.40	1.28	12.48	1.67	11
43	85.20	1.55	0.51	6.25	2.53	32
66	83.68	1.69	0.36	8.75	3.11	45
74	80.33	1.83	0.29	8.86	3.54	54

[a] All elemental analysis values are ±0.3% according to Atlantic Microlab.

[b] The PVC contents of the infiltrated membranes are calculated from the nitrogen and chlorine contents of the electrodes.

Table 2

BET surface area, mesopore surface area, micropore surface area, mesopore volume, micropore volume, and average pore diameter of unoxidized and oxidized 3DOM carbon.

Oxidation time (min)	BET surface area (m^2/g)	Mesopore surface area (m^2/g)[a]	Micropore surface area (m^2/g)	Mesopore volume (cm^3/g)	Micropore volume (cm^3/g)	Average pore diameter (nm)
0	247	25	192	0.031	0.088	1.8
15	372	50	284	0.084	0.160	3.2
60	467	65	354	0.087	0.198	3.1

[a]Mesopore surface area and mesopore volume are calculated for pore size ranges of 1.9–49, 2.1–60 and 2.1–56 nm for 0, 15 and 60 min oxidation, respectively. The difference in the total area/volume and the sum of the mesopore and micropore area/volume are due to pores larger than the upper limit of the mesopore range.

Table 3

Concentrations of the functional groups on the surface of unoxidized and oxidized 3DOM carbon. The E° values of electrodes prepared with oxidized and unoxidized 3DOM carbon solid contacts and polymeric sensing membranes are also shown.

Oxidation time (min)	Ketone (mmol/g)	Phenol (mmol/g)	Lactone and lactol (mmol/g)	Carboxylic acid (mmol/g)[a]	E° (mV)[b]
0	0.34	0.27	0.0	0.0	285±27
10	0.51	0.35	0.35	0.79	531±30
30	0.75	0.50	0.44	1.60	421±19
60	1.05	0.65	0.91	2.72	642±17

[a] The titration method cannot distinguish between carboxylic acid and anhydride groups, which may also be present.

[b] The E° values are an average of three (60 min oxidation) or four (0, 10, and 30 min oxidation) electrodes preparedin an identical manner.

Table 4

Apparent capacitance values obtained for unoxidized and oxidized 3DOM carbon (15 min oxidation) by chronopotentiometry at three different currents.

Sample	Capacitance at 1 mA (F/g)	Capacitance at 0.5 mA (F/g)	Capacitance at 0.1 mA (F/g)
3DOM C	1.92	2.10	2.25
Oxidized 3DOM C	11.0	46.8	68.4

Table 5

Fitting values for the impedance data shown in Figure 4. Labels A to E correspond to Figure 4.

Circuit element	(A) Ni/3DOM C	(B) Ni/PVC	(C) Ni/3DOM C/ PVC	(D) Ni/Ox. 3DOM C [b]/ PVC	(E) Ni/Untempl. C [c]/ PVC
R1 (Ω)	64	-1.1×10^{4}	-1.3×10^{4}	-1.8×10^{4}	-7.5×10^{3}
C1[a] (F)	7.6×10^{-3}	7.7×10^{-11}	5.7×10^{-11}	3.9×10^{-11}	4.8×10^{-11}
R2 (Ω)	1.5×10^{4}	2.8×10^{5}	6.7×10^{5}	7.6×10^{5}	1.1×10^{5}
C2[a] (F)	-	–	8.1×10^{-11}	3.6×10^{-9}	-
R3 (Ω)	-	–	1.8×10^{5}	4.6×10^{4}	-
CPE1-T	1.6×10^{-2}	2.0×10^{-6}	6.1×10^{-6}	2.7×10^{-6}	3.5×10^{-6}
CPE1-P	0.37	0.81	0.53	0.57	0.66
R4 (Ω)	1.1×10^{2}	3.3×10^{6}	-	-	-

[a] C1 and C2 were also fit as CPEs. The CPE phase values indicated the presence of nearly perfect capacitors, so capacitors were used instead.

[b] 3DOM carbon oxidized for 15 min.

[c] Untemplated carbon.